

Isochoric Specific Heat Capacity of Difluoromethane (R32) and a Mixture of 51.11 mass% Difluoromethane (R32)+48.89 mass% Pentafluoroethane (R125)

A. Matsuguchi · K. Yamaya · N. Kagawa

Published online: 18 November 2008
© Springer Science+Business Media, LLC 2008

Abstract The isochoric heat capacity (c_v) of difluoromethane (R32) and a mixture of 51.11 mass% R32+48.89 mass% pentafluoroethane (R125) was measured at temperatures from 268 K to 328 K and at pressures up to 30 MPa. The reported density measurements are in the single-phase region and cover a range of $\rho > 800 \text{ kg} \cdot \text{m}^{-3}$. The measured data are compared with results measured by other researchers. Also, the measured data are examined with available equations of state. As a result, it is found that the measured c_v 's agree well with those of other researchers in the measurement range of the present study.

Keywords Difluoromethane (R32) · Heat capacity · Pentafluoroethane (R125) · $pVTx$ property · R410A

1 Introduction

Recently, chlorofluorocarbon alternatives have attracted attention due to their mild impact on the environment and their high performance. Reliable equations of state for these working fluids are necessary to evaluate the cycle performance of refrigeration systems.

In order to develop a reliable equation of state for a fluid, various thermodynamic property measurements of the fluid are required. Among them, specific isochoric heat capacity (c_v) measurements provide a very useful check for calculations of the second derivative of the pressure, p , with respect to temperature, T , which is essential information to develop equations of state; however, c_v measurements are challenging

A. Matsuguchi (✉) · K. Yamaya · N. Kagawa
Department of Mechanical Systems Engineering, National Defense Academy,
239-8686 Yokosuka, Japan
e-mail: matsu@nda.ac.jp

to measure accurately. Thus, isochoric heat capacity data are, in general, very limited. For the present, difluoromethane (R32, CH₂F₂) and R410A, which is a near azeotropic mixture having 50 mass% R32 and 50 mass% pentafluoroethane (R125, C₂HF₃), are used as refrigerants for refrigerators and heat pumps. For R32 in the compressed liquid phase, earlier measurements of c_v have only been reported by Lüddecke and Magee [1] at temperatures from 250 K to 350 K. For a mixture of 49.99 mass% R32 and 50.01 mass% R125 (R410A), Perkins and Magee [2] have reported c_v results in a temperature range from 300 K to 400 K. To extend and examine these results, isochoric heat capacities of R32 and a mixture of 51.11 mass% R32 and 48.89 mass% R125 were measured. The present measurements have been compared with the earlier c_v measurements in the liquid phase.

In this work, we report c_v and pressure–volume–temperature–composition ($pVTx$) measurements for R32 and R410A and evaluate them with available equations of state at temperatures from 268 K to 328 K, and at pressures up to 30 MPa. The reported density measurements are in the single-phase region and cover a range of $\rho > 800 \text{ kg} \cdot \text{m}^{-3}$.

2 Measurements

2.1 Experimental Procedures

A twin-cell type adiabatic calorimeter was used for these measurements; it has been described previously in detail by Kuroki et al. [3] and Kitajima et al. [4]. A spherical cell (approximately 33 cm³) contains a sample, and a second identical cell serves as a reference. The calorimeter is capable of reaching 470 K. For the heat-capacity measurements, a precisely measured electrical energy (Q) is applied and the resulting temperature rise ($\Delta T = T_2 - T_1$) is measured. c_v is obtained from

$$c_v = \left(\frac{\partial U}{\partial T} \right)_V \cong \frac{\alpha (\Delta Q - \Delta Q_0) - W_{PV}}{m \Delta T} \quad (1)$$

where U is the internal energy, ΔQ_0 is the energy difference between the sample cell and reference cell when both cells are empty, ΔQ refers to the energy added during an experiment with a sample in the sample cell and a blank (vacuum) in the reference cell, W_{PV} is the change-of-volume work due to the slight dilation of the cell, α (determined to be 0.940) is the available electrical energy supplied to the heater wire, and m is the mass of sample in the sample cell.

2.2 Materials

High-purity samples of R32 and R125 were obtained to prepare the mixtures. The R32 was certified to have a minimum purity of 0.9997 mole fraction by gas chromatographic analysis, and the minimum purity of R125 was 0.9990. The mixture of this study was prepared inside the calorimeter cell. A quantity of each pure component was filled into its own lightweight cylinder (75 cm³) and was weighed with a digital balance having

Table 1 Experimental c_v and pVT properties for R32 and 51.11 mass% R32+48.89 mass% R125

T (K)	p (MPa)	ρ (g·cm $^{-3}$)	c_v (J·g $^{-1}$ ·K $^{-1}$)	T (K)	p (MPa)	ρ (g·cm $^{-3}$)	c_v (J·g $^{-1}$ ·K $^{-1}$)
<i>R32</i>							
268.15	8.502	1.0935	0.938	282.15	22.472	1.0914	0.966
269.15	9.512	1.0933	0.955	283.15	23.473	1.0912	0.964
270.15	10.521	1.0932	0.958	284.15	24.472	1.0911	0.960
271.15	11.531	1.0930	0.952	285.15	25.470	1.0909	0.971
272.15	12.540	1.0929	0.943	286.15	26.466	1.0908	0.973
273.15	13.551	1.0927	0.966	287.15	27.461	1.0906	0.965
274.15	14.560	1.0926	0.949	288.15	28.454	1.0904	0.973
275.15	15.568	1.0924	0.951	289.15	29.446	1.0903	0.975
276.15	16.577	1.0923	0.956	268.15	8.268	1.0935	0.951
277.15	17.583	1.0921	0.961	269.15	9.280	1.0933	0.948
278.15	18.589	1.0920	0.951	270.15	10.291	1.0932	0.951
279.15	19.595	1.0918	0.964	271.15	11.302	1.0930	0.950
280.15	20.598	1.0917	0.961	272.15	12.312	1.0929	0.960
281.15	21.601	1.0915	0.959	273.15	13.321	1.0927	0.943
282.15	22.602	1.0914	0.962	274.15	14.330	1.0926	0.960
283.15	23.603	1.0912	0.960	275.15	15.337	1.0924	0.951
284.15	24.606	1.0910	0.966	276.15	16.344	1.0923	0.959
285.15	25.603	1.0909	0.966	277.15	17.350	1.0921	0.948
286.15	26.598	1.0907	0.965	278.15	18.354	1.0920	0.959
287.15	27.594	1.0906	0.968	279.15	19.358	1.0918	0.959
288.15	28.588	1.0904	0.969	280.15	20.361	1.0917	0.954
289.15	29.581	1.0903	0.982	281.15	21.363	1.0915	0.970
272.15	12.421	1.0929	0.972	282.15	22.363	1.0914	0.953
273.15	13.429	1.0928	0.957	283.15	23.363	1.0912	0.969
274.15	14.438	1.0926	0.954	284.15	24.362	1.0911	0.967
275.15	15.444	1.0924	0.958	285.15	25.359	1.0909	0.964
276.15	16.452	1.0923	0.958	286.15	26.356	1.0908	0.971
277.15	17.457	1.0921	0.954	287.15	27.351	1.0906	0.968
278.15	18.462	1.0920	0.966	288.15	28.345	1.0904	0.972
279.15	19.465	1.0918	0.957	289.15	29.338	1.0903	0.970
280.15	20.468	1.0917	0.965	289.15	5.835	1.0159	0.957
281.15	21.470	1.0915	0.954	290.15	6.631	1.0158	0.979
291.15	7.428	1.0157	0.984	290.15	6.570	1.0158	0.973
292.15	8.224	1.0155	0.983	291.15	7.365	1.0157	0.983
293.15	9.019	1.0154	0.994	292.15	8.161	1.0156	0.985
294.15	9.815	1.0153	0.977	293.15	8.956	1.0155	0.988
295.15	10.610	1.0152	0.991	294.15	9.752	1.0153	0.993
296.15	11.405	1.0151	0.990	295.15	10.546	1.0152	0.984
297.15	12.199	1.0149	0.987	296.15	11.341	1.0151	0.984
298.15	12.993	1.0148	0.998	297.15	12.135	1.0150	0.992

Table 1 continued

T (K)	p (MPa)	ρ (g·cm $^{-3}$)	c_v (J·g $^{-1}$ ·K $^{-1}$)	T (K)	p (MPa)	ρ (g·cm $^{-3}$)	c_v (J·g $^{-1}$ ·K $^{-1}$)
299.15	13.787	1.0147	0.996	298.15	12.929	1.0149	0.990
300.15	14.581	1.0146	1.001	299.15	13.723	1.0147	0.993
301.15	15.374	1.0144	0.998	300.15	14.517	1.0146	0.993
302.15	16.167	1.0143	1.004	301.15	15.309	1.0145	1.006
303.15	16.960	1.0142	1.009	302.15	16.102	1.0144	1.001
304.15	17.752	1.0141	1.010	303.15	16.894	1.0142	1.002
305.15	18.543	1.0140	1.011	304.15	17.685	1.0141	1.002
306.15	19.335	1.0138	1.015	305.15	18.476	1.0140	1.014
307.15	20.125	1.0137	1.009	306.15	19.267	1.0139	1.014
308.15	20.915	1.0136	1.015	308.15	20.848	1.0136	1.017
309.15	21.704	1.0134	1.025	309.15	21.639	1.0135	1.013
310.15	22.492	1.0133	1.021	310.15	22.429	1.0134	1.016
311.15	23.281	1.0132	1.032	311.15	23.217	1.0133	1.022
312.15	24.068	1.0131	1.034	312.15	24.005	1.0132	1.031
313.15	24.855	1.0129	1.034	313.15	24.793	1.0130	1.029
314.15	25.641	1.0128	1.027	314.15	25.579	1.0129	1.034
315.15	26.427	1.0127	1.038	315.15	26.364	1.0128	1.030
316.15	27.212	1.0126	1.051	316.15	27.149	1.0127	1.029
317.15	27.996	1.0124	1.042	317.15	27.934	1.0125	1.046
318.15	28.779	1.0123	1.053	318.15	28.719	1.0124	1.040
289.15	5.774	1.0159	0.985				
<i>51.11 mass% R32 + 48.89 mass% R125</i>							
270.15	5.157	1.1901	0.887	269.15	4.259	1.1901	0.891
271.15	5.992	1.1899	0.875	270.15	5.095	1.1899	0.879
272.15	6.828	1.1897	0.879	271.15	5.931	1.1897	0.890
273.15	7.662	1.1895	0.890	272.15	6.767	1.1895	0.898
274.15	8.496	1.1893	0.887	273.15	7.602	1.1893	0.887
275.15	9.328	1.1892	0.886	274.15	8.437	1.1892	0.906
276.15	10.161	1.1890	0.893	275.15	9.272	1.1890	0.902
277.15	10.993	1.1888	0.904	276.15	10.107	1.1888	0.901
278.15	11.824	1.1886	0.895	277.15	10.942	1.1886	0.912
279.15	12.657	1.1884	0.908	278.15	11.776	1.1884	0.911
280.15	13.488	1.1882	0.902	279.15	12.611	1.1882	0.919
281.15	14.319	1.1881	0.913	280.15	13.444	1.1881	0.905
282.15	15.148	1.1879	0.911	281.15	14.277	1.1879	0.926
283.15	15.978	1.1877	0.900	282.15	15.110	1.1877	0.921
284.15	16.808	1.1876	0.918	283.15	15.943	1.1876	0.918
285.15	17.637	1.1874	0.914	284.15	16.775	1.1874	0.922
286.15	18.467	1.1872	0.923	285.15	17.606	1.1872	0.932
287.15	19.297	1.1871	0.906	286.15	18.437	1.1871	0.927
288.15	20.124	1.1869	0.918	287.15	19.268	1.1869	0.927

Table 1 continued

T (K)	p (MPa)	ρ ($\text{g} \cdot \text{cm}^{-3}$)	c_v ($\text{J} \cdot \text{g}^{-1} \cdot \text{K}^{-1}$)	T (K)	p (MPa)	ρ ($\text{g} \cdot \text{cm}^{-3}$)	c_v ($\text{J} \cdot \text{g}^{-1} \cdot \text{K}^{-1}$)
289.15	20.951	1.1868	0.921	288.15	20.097	1.1868	0.935
290.15	21.778	1.1866	0.919	289.15	20.926	1.1866	0.927
291.15	22.607	1.1865	0.918	290.15	21.755	1.1865	0.935
292.15	23.433	1.1864	0.926	291.15	22.583	1.1863	0.927
293.15	24.257	1.1862	0.920	292.15	23.410	1.1862	0.936
294.15	25.082	1.1861	0.935	293.15	24.236	1.1860	0.932
295.15	25.903	1.1859	0.904	294.15	25.062	1.1859	0.937
296.15	26.725	1.1858	0.924	295.15	25.887	1.1857	0.933
297.15	27.546	1.1856	0.920	296.15	26.711	1.1856	0.931
298.15	28.366	1.1855	0.910	297.15	27.534	1.1855	0.926
299.15	29.186	1.1854	0.918	298.15	28.357	1.1853	0.929
300.15	30.003	1.1852	0.927	299.15	29.179	1.1852	0.938
268.15	3.423	1.1903	0.875	300.15	29.999	1.1851	0.911
270.15	5.065	1.1899	0.887	297.15	6.292	1.0977	0.947
271.15	5.903	1.1897	0.902	298.15	6.917	1.0976	0.942
272.15	6.740	1.1896	0.892	299.15	7.541	1.0974	0.935
273.15	7.576	1.1894	0.897	300.15	8.166	1.0972	0.946
274.15	8.411	1.1892	0.905	301.15	8.791	1.0971	0.944
275.15	9.245	1.1890	0.902	302.15	9.417	1.0969	0.931
276.15	10.082	1.1888	0.914	303.15	10.042	1.0968	0.934
277.15	10.917	1.1886	0.915	304.15	10.667	1.0967	0.938
278.15	11.753	1.1884	0.918	305.15	11.292	1.0965	0.918
279.15	12.587	1.1882	0.913	306.15	11.917	1.0964	0.920
280.15	13.423	1.1881	0.930	307.15	12.541	1.0962	0.930
281.15	14.258	1.1879	0.913	308.15	13.165	1.0961	0.915
282.15	15.091	1.1877	0.930	309.15	13.790	1.0959	0.919
283.15	15.926	1.1875	0.926	310.15	14.414	1.0958	0.916
284.15	16.759	1.1874	0.925	311.15	15.038	1.0957	0.915
285.15	17.592	1.1872	0.934	312.15	15.662	1.0955	0.907
286.15	18.423	1.1871	0.928	313.15	16.286	1.0954	0.907
287.15	19.253	1.1869	0.920	314.15	16.910	1.0953	0.907
288.15	20.083	1.1867	0.936	315.15	17.534	1.0951	0.897
289.15	20.914	1.1866	0.936	316.15	18.158	1.0950	0.902
290.15	21.743	1.1864	0.938	317.15	18.781	1.0949	0.896
291.15	22.571	1.1863	0.935	318.15	19.404	1.0948	0.893
292.15	23.400	1.1862	0.936	319.15	20.027	1.0946	0.898
293.15	24.226	1.1860	0.933	320.15	20.649	1.0945	0.894
294.15	25.053	1.1859	0.937	321.15	21.272	1.0944	0.884
295.15	25.878	1.1857	0.929	322.15	21.894	1.0943	0.890
296.15	26.704	1.1856	0.944	323.15	22.516	1.0942	0.884
297.15	27.528	1.1855	0.935	324.15	23.137	1.0940	0.870

Table 1 continued

T (K)	p (MPa)	ρ ($\text{g} \cdot \text{cm}^{-3}$)	c_v ($\text{J} \cdot \text{g}^{-1} \cdot \text{K}^{-1}$)	T (K)	p (MPa)	ρ ($\text{g} \cdot \text{cm}^{-3}$)	c_v ($\text{J} \cdot \text{g}^{-1} \cdot \text{K}^{-1}$)
298.15	28.352	1.1854	0.931	325.15	23.758	1.0939	0.877
299.15	29.176	1.1852	0.939	326.15	24.379	1.0938	0.872
300.15	29.998	1.1851	0.925	327.15	25.000	1.0937	0.885
296.15	5.667	1.0979	0.915	328.15	25.620	1.0936	0.864
296.15	5.620	1.0979	0.953	296.15	5.585	1.0979	0.965
297.15	6.246	1.0977	0.957	297.15	6.213	1.0977	0.955
298.15	6.872	1.0975	0.949	298.15	6.841	1.0975	0.974
299.15	7.499	1.0974	0.963	299.15	7.469	1.0974	0.960
300.15	8.124	1.0972	0.943	300.15	8.097	1.0972	0.961
301.15	8.750	1.0971	0.946	301.15	8.725	1.0971	0.953
302.15	9.377	1.0969	0.957	302.15	9.353	1.0969	0.947
303.15	10.003	1.0968	0.949	303.15	9.980	1.0968	0.953
304.15	10.629	1.0966	0.930	304.15	10.607	1.0966	0.955
305.15	11.256	1.0965	0.937	305.15	11.234	1.0965	0.930
306.15	11.881	1.0964	0.931	306.15	11.861	1.0964	0.947
307.15	12.507	1.0962	0.935	307.15	12.487	1.0962	0.928
308.15	13.133	1.0961	0.936	308.15	13.114	1.0961	0.932
309.15	13.758	1.0959	0.933	309.15	13.740	1.0959	0.930
310.15	14.384	1.0958	0.918	310.15	14.367	1.0958	0.933
311.15	15.009	1.0957	0.920	311.15	14.992	1.0956	0.924
312.15	15.634	1.0955	0.933	312.15	15.618	1.0955	0.902
313.15	16.259	1.0954	0.920	313.15	16.243	1.0954	0.927
314.15	16.883	1.0952	0.917	314.15	16.869	1.0952	0.920
315.15	17.507	1.0951	0.915	315.15	17.493	1.0951	0.914
316.15	18.131	1.0950	0.905	316.15	18.118	1.0950	0.914
317.15	18.755	1.0949	0.894	317.15	18.743	1.0949	0.910
318.15	19.379	1.0947	0.902	318.15	19.367	1.0947	0.903
319.15	20.003	1.0946	0.905	319.15	19.990	1.0946	0.904
320.15	20.627	1.0945	0.914	320.15	20.613	1.0945	0.886
321.15	21.250	1.0944	0.899	321.15	21.236	1.0944	0.899
322.15	21.873	1.0943	0.888	322.15	21.858	1.0942	0.899
323.15	22.495	1.0941	0.888	323.15	22.480	1.0941	0.888
324.15	23.117	1.0940	0.903	324.15	23.103	1.0940	0.894
325.15	23.738	1.0939	0.881	325.15	23.725	1.0939	0.893
326.15	24.361	1.0938	0.902	326.15	24.347	1.0938	0.894
327.15	24.981	1.0937	0.877	327.15	24.970	1.0937	0.886
328.15	25.601	1.0936	0.877	328.15	25.590	1.0936	0.875

0.1 mg uncertainty. After both components of the mixture were introduced into the cell from its cylinder, the cell was cooled below 278 K by a mini-cooler. The remaining mass in each cylinder was weighed, and the composition of the sample in the cell

was calculated from the mass charged to the cell. The R410A composition in this study consists of 51.11 mass% R32 and 48.89 mass% R125 which is slightly shifted from the nominal composition of R410A (50 mass% R32 and 50 mass% R125). To ensure complete homogenization prior to measurements, the sample temperature was rapidly increased until the sample pressure reached 20 MPa, then it was cooled, and this process was repeated.

2.3 Assessment of Uncertainties

The experimental expanded uncertainty (with a coverage factor $k = 2$) of the absolute temperature measurement is ± 13 mK, by considering the calibration report of the PRTs (± 2 mK), temperature gradients in the cell, and the accuracy of each instrument. The value for the pressure measurement for $k = 2$ is ± 8 kPa, based on the pressure transducer specifications and the accuracy of the instruments. The standard uncertainty of the inner volume of the cell is 0.025 cm^3 , estimated by calibration with distilled water, and that of the mass measurement is 0.15 mg , based on balance specifications and the standard uncertainty of the air buoyancy effect. The estimated expanded uncertainty of the density is $\pm 0.16 \%$, as derived from the standard uncertainties of the inner volume of the cell and the mass measurement. The expanded uncertainty of c_v is estimated from a combination of the standard uncertainty of the elapsed time required for a 1 K temperature rise (0.65 %), that of the change-of-volume work (20 %) which contributes 0.3 % to the uncertainty of c_v , the experimental standard deviation of α of 0.6 %, the uncertainty of the density, and the temperature fluctuation of adiabatic shields which contributes an amount of $0.4/(mc_v) \text{ J} \cdot \text{g}^{-1} \cdot \text{K}^{-1}$ to the uncertainty of c_v . The resulting expanded uncertainty ($k = 2$) of c_v is $\pm 3.2 \%$ in the liquid.

3 Results

The experimental c_v and $pVTx$ results at temperatures spaced by 1 K for R32 and R410A are presented in Table 1. The data for each system are measured along two isochores. Figure 1 shows the density deviations for the pVT measurements for R32 from an equa-

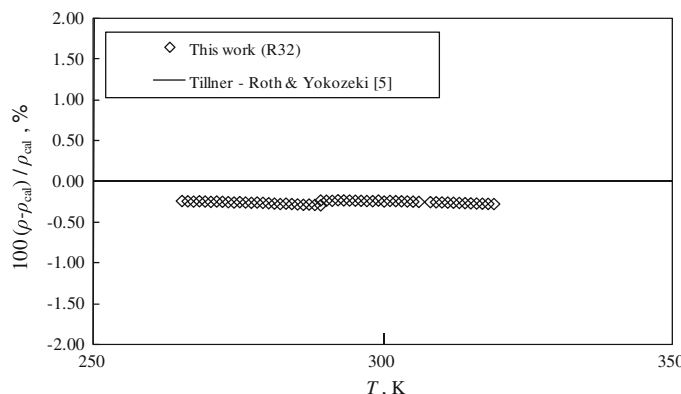


Fig. 1 Deviations of measured densities for R32 with an EOS by Tillner-Roth and Yokozeki [5]

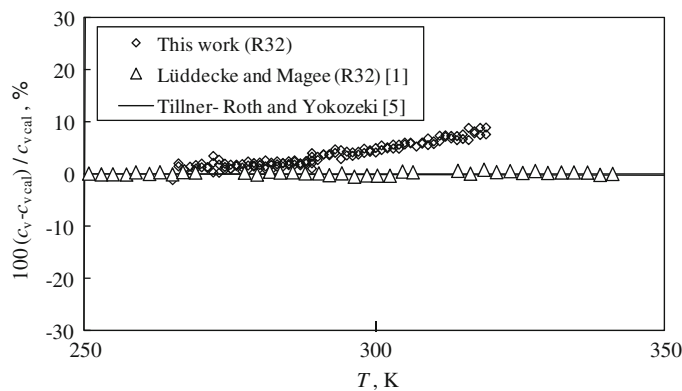


Fig. 2 Deviations of measured c_v for R32 from calculations with an EOS by Tillner-Roth and Yokozeki [5]

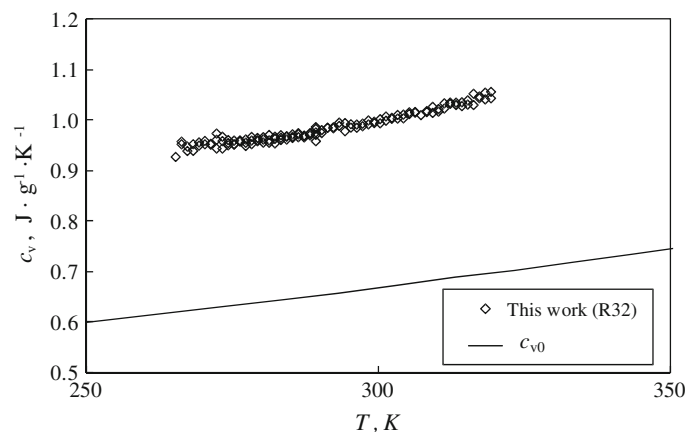


Fig. 3 Isochoric heat capacities for R32 at liquid-phase states

tion of state (EOS) developed by Tillner-Roth and Yokozeki [5]. The model represents most published pVT data [5] within the measurement uncertainty. The present data are represented within 0.3 % over the temperature range of the measurements. The largest deviation is about double the measurement uncertainty. However, these deviations do not have a large influence on the c_v measurements, because the uncertainty of the density does not contribute to the uncertainty of c_v greatly. Figure 2 shows deviations of the present c_v data from the EOS. Also, the data reported by Lüddecke and Magee [1] are plotted in this figure. The model represents the published data quite well. Because the c_v data were fitted simultaneously with other thermodynamic property data including pVT measurements, it is very important to confirm whether all of the data distributed widely and uniformly. Figure 3 shows the behavior of the present c_v data of R32, and the calculated specific heat capacity of the ideal gas, c_{v0} , by using the EOS. At temperatures below 290 K, the present data agree with the EOS and the data by Lüddecke and Magee within the expanded uncertainty. However, at temperatures

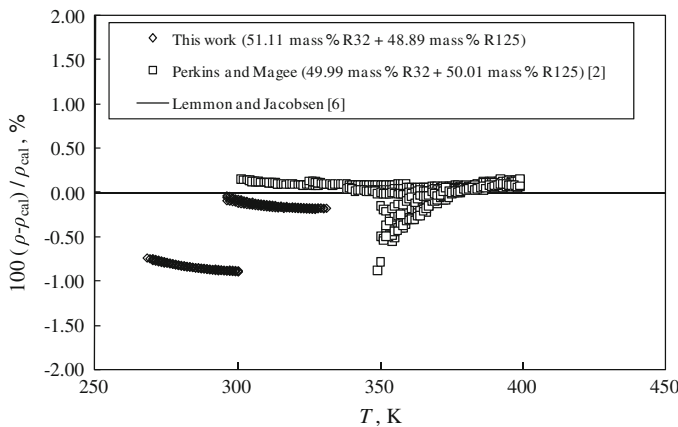


Fig. 4 Deviations of measured densities for R410A from calculations with a mixing rule by Lemmon and Jacobsen [6]

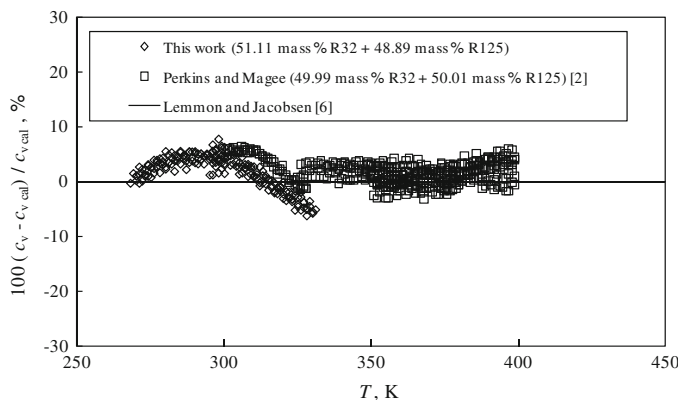


Fig. 5 Deviations of measured c_v for R410A from calculations with a mixing rule by Lemmon and Jacobsen [6]

above 290 K the present data are higher than the calculated EOS values. The reason for the deviations from the published data in this temperature region is not clear.

Figure 4 shows density deviations for the $pVTx$ measurements from calculated values with a mixing rule developed by Lemmon and Jacobsen [6] for mixture predictions. Also, the data measured with a calorimeter by Perkins and Magee [2] are compared in this figure. The present data are represented within $\pm 1.0\%$ in the temperature range of the current measurements. Figure 5 shows the deviations of the present c_v data from the calculated values [6]. Figure 6 shows the behavior of the present c_v data, and calculated c_{v0} [6]. Also, the data reported by Perkins and Magee [2] are superimposed in Figs. 5 and 6. The present c_v data for $\rho = 1.19 \text{ g} \cdot \text{cm}^{-3}$ from 268 K to 300 K and $\rho = 1.09 \text{ g} \cdot \text{cm}^{-3}$ from 301 K to 328 K agree well with the calculated values within the expanded experimental uncertainty as well as the data for $\rho = 1.07 \text{ g} \cdot \text{cm}^{-3}$ from 301 K to 328 K reported by Perkins and Magee.

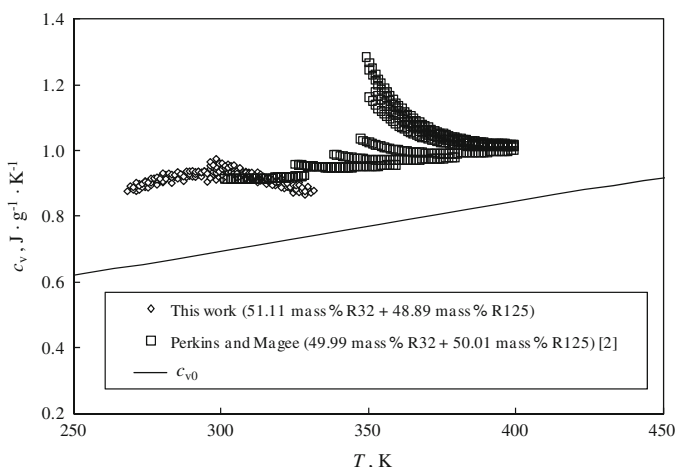


Fig. 6 Isochoric heat capacities for R 410A at liquid-phase states

4 Conclusions

Measurements of c_v and $pVTx$ properties were reported for R32 and the mixture of 51.11 mass% R32 and 48.89 mass% R125 in the liquid phase. The published equations of state represent the observed behavior of c_v measurements over this measurement range. These data will be essential to develop new accurate equations of state to represent thermodynamic properties of the binary mixture.

References

1. T.O. Lüddecke, J.W. Magee, Int. J. Thermophys **17**, 823 (1999)
2. R.A. Perkins, J.W. Magee, J. Chem. Eng. Data **50**, 1727 (2005)
3. T. Kuroki, N. Kagawa, H. Endo, S. Tsuruno, J.W. Magee, J. Chem. Eng. Data **46**, 1101 (2001)
4. H. Kitajima, N. Kagawa, S. Tsuruno, K. Watanabe, Int. J. Thermophys. **26**, 1733 (2005)
5. R. Tillner-Roth, A. Yokozeki, J. Phys. Chem. Ref. Data **25**, 1273 (1997)
6. E.W. Lemmon, R.T. Jacobsen, J. Phys. Chem. Ref. Data **33**, 593 (2004)